International Journal of Industrial Engineering Computations 16 (2025) 177–196

Contents lists available at GrowingScience

International Journal of Industrial Engineering Computations

homepage: www.GrowingScience.com/ijiec

Research on storage location allocation in three-dimensional automated warehouse based on cargo damage control

Qianli Ma[a,b], Linlin Xu[b], Lin Zhu[a,b] and Peng Jia[a,b*]

[a]*Collaborative Innovation Center for Transport Studies, Dalian Maritime University, Dalian, 116026, China*
[b]*School of Maritime Economics and Management, Dalian Maritime University, Dalian, 116026, China*

CHRONICLE

Article history:
Received June 3 2024
Received in Revised Format September 16 2024
Accepted October 9 2024
Available online October 9 2024

Keywords:
Storage location allocation
Cargo damage
Travel efficiency
SPEA-II algorithm

ABSTRACT

In automated high-bay warehouses, the results of storage location allocation significantly impact the operational efficiency of subsequent warehouse operations. Considering that cargo loss within the warehouse is often caused by contact with equipment, this paper proposes an innovative dual-objective optimization model aimed at minimizing unit cargo loss and the average travel time of stacker cranes through rational storage allocation. The study's findings indicate that different cargo sizes, shelf sizes, and operational modes have varying degrees of impact on stacker crane operational efficiency and cargo loss. A reasonable match between equipment and product sizes helps enterprises minimize space waste, expedite response to customer demands, and reduce operational costs. This study optimizes storage location allocation using the SPEA-II algorithm and performs a comprehensive comparison with the results from CPLEX and NSGA-II. The results demonstrate that the SPEA-II algorithm performs excellently across various problem scales, indicating that it is an effective method for solving storage location allocation issues.

1. Introduction

As an important node of logistics activities, the warehouse plays the function of goods storage and circulation (Frazelle, 2002). The evolution of the Internet has created conducive conditions for the facilitation of online shopping, leading to a paradigm shift in customer orders characterized by small batches and a diverse range of products (Liu et al., 2016; 2021; Liu and Kim, 2023; Jiao et al., 2024). In addition, as consumers and the market for warehouse demand response speed continues to increase, it is particularly vital to improve the efficiency of outbound picking of goods (Chiu et al., 2019; Samira, 2022). In order to expeditiously address consumer demands, warehouses necessitate the efficient and accurate execution of order picking processes (Zhong et al., 2022).

Previous warehouses relied on manual work, causing errors, slow operations, and poor space use. The researchers conducted a comparative analysis of warehouses with different layout types and found that a rational layout can effectively reduce the picking path lengths (Ozden et al., 2020; Esmer et al., 2013). The advent of automated three-dimensional warehouses powered by AS/RSs revolutionized logistics. These warehouses offer efficiency and optimization, overcoming manual limitations (Liu et al., 2018; Bartholdi and Hackman, 2015). Automated systems ensure rapid, accurate responses to customers and precise internal operations (Sari et al., 2007; Rose et al., 2021). Fig. 1 shows the warehouse's layout and key components.

* Corresponding author Tel: +86 19862175223
E-mail 2358453249@qq.com (P. Jia)
ISSN 1923-2934 (Online) - ISSN 1923-2926 (Print)
2025 Growing Science Ltd.
doi: 10.5267/j.ijiec.2024.10.003

(a) Automated warehouse (b) Crane (c) Conveyor

Fig. 1. AS/RS system

When the order arrives at the warehouse, the stacker crane needs to shuttle through the roadway according to the order information for goods picking. During the goods retrieval and outbound phase, the goods are retrieved by a stacker crane, placed on a conveyor belt, and then moved to the picking station (Hoshimov et al., 2022).The phase of order picking, being the most labor-intensive segment, approximately constitutes 50% of the total order fulfillment duration, and the processing costs associated with this specific task significantly contribute to the overall operational costs of the warehouse, ranging prominently between 50% and 75% (Tompkins et al., 2010; Frazelle, 2000; Grosse et al., 2015). For business operators, effective warehouse management should feature rapid demand response, high operational accuracy and low costs (Womack et al., 1990; Abdirad & Krishna, 2021). Thus, enterprises must consider strategies to boost warehouse proficiency.

Storage location allocation is crucial for order picking efficiency and cost-effectiveness (Franzke et al., 2017). A smart allocation improves space utilization and reduces inventory checking time (Tokat et al., 2022). And it also minimizes crane travel and operational costs (Mirzaei et al., 2021). Factors like goods turnover and variety impact allocation outcomes (Lam et al., 2010). With increasing consumer and market demands, the aim of the warehouse is to maximize operational efficiency or minimize costs (Accorsi et al., 2012, 2014).

In complex automated three-dimensional warehouses, the outcomes of storage location allocation significantly impact subsequent process efficiency and overall operational costs. Beyond focusing on the critical metric of stacker crane operational time, this paper also incorporates the cost of merchandise loss due to crane operations. By employing the SPEA-II and NSGA-II algorithms to solve and compare the dual-objective problem, the study better captures the conflicts between different objectives. The results indicate that considering both cost and efficiency from a holistic perspective enhances overall warehouse performance, improves customer satisfaction, and strengthens warehouse competitiveness. The methods used in this paper underscore the strategic importance of optimizing storage location allocation in modern warehousing systems.

2 Literature review

2.1 Automated three-dimensional warehouses and space allocation strategies

Automated three-dimensional warehouses use AS/RSs, internet tech, stacker cranes and conveying systems to process online orders (Lagorio et al., 2022). Common storage strategies include positioning, classified, random, and joint (Francis et al., 1992). Positioning assigns items to fixed locations. Classified organizes by characteristics, random lacks order, and joint combines for spatial efficiency. The strategy chosen affects retrieval, utilization, and efficiency, vital in automated warehouses.

Given the increased storage capacity of these warehouses compared to non-automated counterparts, employing a random storage assignment policy may necessitate pickers or stackers reaching multiple storage locations for tasks (Manzini, 2012). Moon and Kim (2001) and Liao et al. (2022) compared the utilization rates of warehouse storage space and replenishment efficiency under different storage strategies respectively. The studies revealed that while random storage improves the utilization rate of free storage space, it can lead to the inefficient occupation of optimal storage space. Bozer and Aldarondo (2018) compared the expected retrieval time using two different order picking systems for the same set of customer orders. Pawar et al. (2022) noted that storage location assignment strategies, coupled with changes in warehouse shelf layout, result in significant variations in operational time for both warehouse equipment and employees.

2.2 Storage space optimization

By analyzing a certain number of orders in a certain period of time, it is found that the probability of certain types of goods appearing in the same order at the same time is high, which means that the demand for these goods shows a certain correlation (Xiang et al., 2018). In addition, the frequency of different types of goods in and out of the warehouse is not exactly the same, and the goods with high frequency of entry and exit have a greater impact on the running distance of the stacker crane (Mirzaei et al., 2021; Guan and Li, 2018; Xiao and Zheng, 2012). Lee et al. (2020) built a mathematical model and solved it for the purpose of minimizing warehouse working time. The need for warehouse outbound operation is increasing and the operation is more complex, so it is necessary to sort or batch the order and access tasks (Li et al., 2017a). Many scholars studied the integrated optimization of storage space allocation, order batching and picking path (Yang et al., 2020; Zhang et al., 2019).

Some relevant studies arranged the cargo storage location or picking order on the basis of optimizing the picking path of goods in the warehouse (Xiang et al., 2018; Li et al., 2017b). Van et al. (2019) proposed a mixed integer programming model considering picking time and solved the model by local search. Yang and Thi (2016) employed a storage allocation strategy based on constraints associated with item-item and item-location relationships.

Table 1
Overview of papers using the storage allocation strategy

Authors	Order batching	Cargo loss	Objectives
Xiang et al. (2018)	yes	no	order association
Xiao and Zheng (2012)	no	no	number of picks
Mirzaei et al. (2021)	no	no	travel efficiency
Guan and Li (2018)	no	no	number of picks
Li et al. (2017a)	yes	no	travel distance
Yang et al. (2020)	yes	no	travel distance
Xiang et al. (2018)	yes	no	number of picks
Li et al. (2017b)	no	no	travel efficiency
Van et al. (2019)	yes	no	travel efficiency
Yang and Thi (2016)	no	no	travel efficiency
Lee et al. (2020)	no	no	travel efficiency and traffic flow balance
Zhang et al. (2019, 2020)	no	no	travel efficiency and delivery cost

2.3 Cost of cargo damage in warehouses

Goods, especially perishable items, naturally experience quality attenuation during storage (Maxim et al., 2016). This decay influences buyers' willingness to purchase and reduces the likelihood of goods leaving the warehouse (Rong et al., 2011). Consequently, optimization objectives for subsequent product scheduling, as proposed by Lütke et al. (2005) and Myers (1997), include considerations for product decay and incorporate product shelf life as a constraint. Beyond cargo damage due to inherent quality decay, the loading and unloading process of the stacker crane involves direct contact with goods, resulting in some degree of loss. Events such as goods dumping during transportation further contribute to losses, elevating warehouse costs (Silve et al., 2020). Recognizing the correlation between actual cargo damage costs and the distance traveled by stacker cranes, Guerriero et al. (2015) incorporated operating costs associated with moving goods into cargo storage arrangements. Prior studies overlooked costs related to equipment operations and goods losses. Cargo damage costs, especially for high-value goods, can significantly impact overall efficiency. This paper proposes a storage optimization model to enhance operational efficiency and consider cargo loss costs. It aims to improve storage allocation, reduce costs, and enhance warehouse competitiveness.

3. Description of the problem

In the automated three-dimensional warehouse, each shelf aisle is equipped with a stacker crane. These stacker cranes operate individually, handling either inbound or outbound storage for a specific type of goods. Each stacker crane is responsible for warehousing operations on both sides of the same aisle. The warehouse configuration, depicted in Fig. 2, reveals a global top view and a side view of selected shelves.

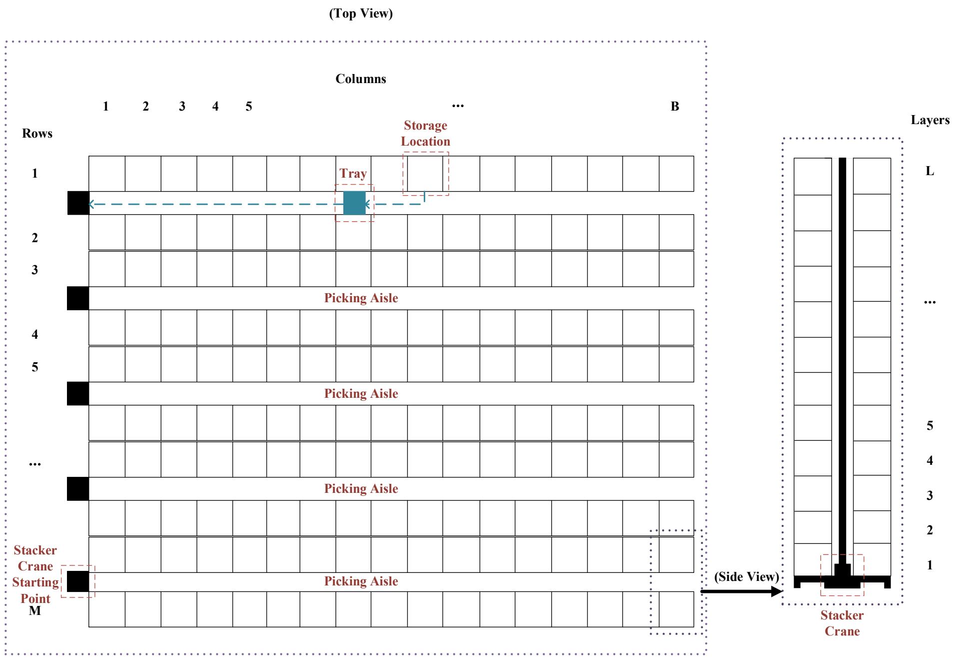

Fig. 2. Automated three-dimensional warehouse layout

The warehouse comprises M rows of shelves, each with B columns and L layers, resulting in a total available storage space of J. Each storage location is identified by a unique three-dimensional coordinate, where each of the three values denotes the row, column, and layer of the storage location. Notably, coordinates where each ordinate is equal to 0 and the altitude coordinate is equal to 1 represent the starting point for stackers in different aisles. The storage facility accommodates I kinds of goods, each with a quantity Q_i. This study incorporates factors such as the risk of goods damage and entry/exit frequency. Subsequently, a multi-objective storage location allocation optimization model is developed to enhance warehouse operational efficiency.

4. Model establishment

4.1 Model conditions assumptions

(1) The dimensions of each cargo space are the same, and the length, width and height of the cargo space are known;
(2) The stackers are located at the same end of the shelves;
(3) The stacker simultaneously moves along the horizontal and vertical direction with constant velocity v and v is known;
(4) The time for the stacker to access the goods is ignored;
(5) The stacking height of each type of goods on the pallet does not exceed the storage location height;
(6) The center of gravity of every type of cargo is located at the geometric center of the storage location;
(7) The unit value of each type of goods in each cycle remains unchanged;
(8) All storage slots in the warehouse are empty and available.

4.2 Parameters and variable settings

The following notations are used in this paper:

Indices

i	index of item, $i \in \{1,...,I\}$
j	auxiliary index, $j \in \{1,...,I\}$

Parameters

l	length of the storage space (unit: meter)
h	height of the storage space (unit: meter)
w	width of the storage space (unit: meter)
M	number of rows of shelves
B	number of columns of shelves
L	number of layers of shelves
J	total number of storage location in warehouse
I	total number of goods categories
t	a work cycle of the warehouse (unit: day)
p_i	times of item i in and out of the warehouse in a day (unit: times)
v	the speed of the stacker (unit: meter/second)
c_i	unit value of item i (unit: RMB cents)
α_i	cargo damage rate per unit distance of item i (unit: damage rate/meter)
D_i	total quantity of cargo loss of item i
T_{it}	the total number of times item i is shelved or retrieved within time period t (unit: times)
Q_i	the quantity of item i before each time it is put on the shelf
d_i	the total moving distance of the item I (unit: meter)
d_{oi}	the distance from the position of storage location of item i to the I/O point (unit: meter)
t_{oi}	the travel time required from the storage location of item i to the I/O point (unit: second)
t_i	the travel time required for a single movement of item i (unit: second)

Decision variables

x_i	the shelf row number of storage location i
y_i	the shelf column number of storage location i
z_i	the shelf layer number of storage location i

Auxiliary variable

δ_{ij}	if the coordinates of goods i and j are the same it is 0, otherwise it is 1

4.3 Establish a multi-objective storage location optimization model

(1) Minimize the cost of unit cargo damage in a cycle

Operational costs of the warehouse include crane operations and cargo loss. Cargo loss increases with goods quantity and price, often due to crane contact. Strategic storage positioning reduces cargo loss by optimizing crane operations. This paper measures cargo loss using the unit distance per unit cargo loss rate in crane operations. Subsequently, the cost of unit cargo loss is calculated based on this metric. The established objective function is outlined as follows:

$$\min F_1 = \frac{\sum_{i=1}^{I} c_i \times D_i}{\sum_{i=1}^{I} Q_i} \tag{1}$$

$$D_i = \alpha_i \times d_i \times Q_i \tag{2}$$

The coordinates of item i are represented as (x_i, y_i, z_i), while the corresponding starting point coordinates of the stacker are $(x_i, 0, 1)$. Consequently, the distance from the position of item i to the starting point of its respective stacker can be calculated as:

$$d_{oj} = \sqrt{(y_i \times l)^2 + ((z_i - 1) \times h)^2} \tag{3}$$

$$d_i = T_{it} \times d_{oj} \times x_{ij} \tag{4}$$

$$T_{it} = p_i \times t \tag{5}$$

(2) Minimize the stacker operation time for unit cargo

Stacker crane operational duration is key to warehouse efficiency, reflecting storage allocation. This study improves the metric by considering crane time per unit goods, reflecting allocation effectiveness.

$$\min F_2 = \frac{\sum_{i=1}^{I} \left(t_i \times T_{it}\right)}{\sum_{i=1}^{I} Q_i} \tag{6}$$

The stacker crane moves horizontally and vertically simultaneously. Additionally, its "single access" operational mode doubles the distance and time for storing or retrieving goods.

$$t_{oi} = \frac{d_{oi}}{v} \tag{7}$$

From Eq. (1) to Eq. (7), the storage location optimization model can be obtained as follows:

$$\min F_1 = \frac{\sum_{i=1}^{I} c_i \times D_i}{\sum_{i=1}^{I} Q_i} \tag{1}$$

$$\min F_2 = \frac{\sum_{i=1}^{I} \left(t_i \times T_{it}\right)}{\sum_{i=1}^{I} Q_i} \tag{6}$$

subject to

$$1 \le x_i \le M, \text{ and } x_i \text{ is a positive integer} \tag{8}$$

$$1 \le y_i \le B, \text{ and } y_i \text{ is a positive integer} \tag{9}$$

$$1 \le z_i \le L, \text{ and } z_i \text{ is a positive integer} \tag{10}$$

$$x_i - x_j + M \times \delta_{ij} \ge 1 \tag{11}$$

$$y_i - y_j + M \times \delta_{ij} \ge 1 \tag{12}$$

$$z_i - z_j + M \times \delta_{ij} \ge 1 \tag{13}$$

$$\delta_{ij} \in \{0,1\} \tag{14}$$

Eq. (8), Eq. (9) and Eq. (10) represent the range of the decision variables, meaning that the storage location of each type of goods cannot exceed the number of rows, columns, and layers of the warehouse shelves. Eq. (11), Eq. (12), and Eq. (13) indicate that goods *i* and *j* cannot be assigned to the same storage location. In these equations, M is an extremely large value. Eq. (14) indicates that δ_{ij} is a binary variable. When it equals 0, it indicates that the coordinates of goods *i* and *j* are exactly the same, meaning they are assigned to the same storage location. When it equals 1, it indicates that the coordinates of goods *i* and *j* are different, meaning they are assigned to different storage locations.

5. SPEA-II Algorithm description

The study explores how cargo storage allocation impacts warehouse operations, considering stacker crane operation time and total cargo loss cost. While converting multi-objective problems into single-objective ones via weighting simplifies solving, challenges arise in assigning weights. Single-objective solutions limit comprehensive evaluation and comparison, hindering full problem understanding. In contrast, multi-target optimization considers target interrelationships, offering a range of optimal solutions representing various trade-offs, aiding decision-making (Hohmann et al., 2022; Zhang & Shi, 2024).

5.1 SPEA-II algorithm introduction and implementation steps

5.1.1 Algorithm introduction

The SPEA-II algorithm is a multi-objective optimization algorithm based on Pareto dominance relation, which aims to solve the optimization problem with multiple conflicting targets. It combines strategies such as Pareto dominance relations, external populations, and density estimation to find a set of equilibrium solutions between multiple objective functions.

5.1.2 Implementation steps

The pseudocode of the SPEA-II algorithm is shown in Table 2.

Table 2
Pseudocode for the SPEA-II algorithm

```
Input:
    N̄ - Population size
    S - Maximum number of iterations
    convergence_threshold - Convergence threshold
    P0 - Initial population
Output:
    A-archive
    Initialize population
    P = P0
    A0 = empty_archive()
    iteration = 0
    A = A0
    while not convergence_criteria_met(iteration, S, convergence_threshold) do:
        evaluate_population(problem, P)
        A = update_external_archive(A0, P)
        N = environmental_selection(P ∪ A)
        selected_parents = mating_selection(N)
        offspring = crossover_and_mutation(selected_parents)
        P = replace_population(P, offspring)
        iteration = iteration + 1
      return archive
```

5.2 Algorithm initialization preparation

5.2.1 Chromosomal encoding

According to the characteristics of the warehouse storage optimization model, the real number coding method is selected in SPEA-II algorithm. The chromosome is constructed by the storage location code where the goods are located, that is, each storage location code is a gene. The three-digit number of the number from left to right represents the value of x_i, y_i and z_i in turn, each chromosome includes $3 \times I$ genes, where I represents the number of types of goods to be stored. And the specific coding form of chromosomes is shown in Fig. 3.

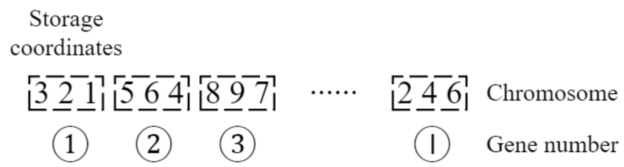

Fig. 3. Chromosomal coding form

5.2.2 Initialize the population

Initializing the population is to randomly generate a three-dimensional matrix of $3 \times I$ columns in $\bar{N}$ rows, where $\bar{N}$ is the population size. Each chromosome represents a storage site allocation scheme in the population. To ensure uniqueness, chromosomes are examined individually, and if duplicate cargo locations are found, their coordinates are randomly regenerated until all cargo locations are distinct.

5.3 Fitness assignment

In order to avoid the occurrence of individuals who are governed by the same external profile members with the same fitness values, in the SPEA-II algorithm, the solution dominated by each individual and the solution that governs it are taken into account. Both population P and individual f in the external profile are given a strength $S(f)$, which indicates the number of solutions that are governed by that individual. On the basis of $S(f)$, the original fitness value $R(f)$ of all individuals in the population and external archives is calculated, where $R(f)$ is equal to the sum of the intensity values of all individuals who dominate the individual. The smaller the original fitness value, the less the solution that dominates the individual, and the better the solution. For individuals with the same original fitness values, as shown in equation (15), the individual density value $D(f)$ was calculated by employing the k-immediate proximity method to distinguish between individuals. In this equation, σ_f^k represents the Euclidean distance between the individual f and the k-*th* neighbor in P_{t+1}. Equation (16) illustrates how k is calculated.

$$D(f) = \frac{1}{\sigma_f^k + 2} \tag{15}$$

$$k = \sqrt{N + \bar{N}} \tag{16}$$

Finally, as shown in Eq. (17), the individual's fitness value $F(f)$ is the sum of the original fitness value and the density value.

$$F(f) = D(f) + R(f) \tag{17}$$

5.4 External archive maintenance

Since the size of the external archive is always N, the file maintenance can retain the high-quality solution and improve the global search ability of the algorithm. The steps to perform external archive maintenance are as follows:

Step1: Copy all non-inferior decompositions from population P_t and external archive A_t into $/A_{t+1}/$, accepted if $/A_{t+1}/=N$;
Step2: If $/A_{t+1}/<N$, then N- $/A_{t+1}/$ is selected from the dominated solution of P_t and A_t and put into A_{t+1};
Step3: If$/A_{t+1}/>$N, then find the smallest crowding distance individual from A_{t+1} and remove it until $/A_{t+1}/=N$, if the minimum distance between the two individuals and the other individuals is equal, then the proximal distance is considered, i.e., k=2.

The robust parameter configurations of SPEA-II make it suitable for diverse multi-objective optimization challenges.

6. Empirical Analysis

In order to verify the validity of the model and algorithm, this paper uses the commercial software IBM ILOG CPLEX 12.8.0 and Python 3.10 to design the algorithm program and sets the maximum running time of CPLEX to 5 hours. When designing the SPEA-II algorithm using Python 3.10.

6.1 Case Description

The Joyi Supply Chain Management Limited Company is a large-scale comprehensive enterprise focusing on modern logistics and supply chain services. The company is customer-oriented, providing warehousing products, transportation and distribution products, integrated supply chain solutions, and various value-added services. After receiving the customer's order, the stacker cranes in the automated three-dimensional warehouse start to run, they will pick accordingly according to the commodity material number and the quantity demanded, and then place the picked goods on the conveyor belt, which will be packaged by the specialized staff, and then transported out of the warehouse and safely delivered to the consumers. The shelving size and operating parameters of the equipment in the warehouse are listed in Table 3. The basic information of multiple types of products is extracted from the real data of the warehouse, including quantity, inbound and outbound frequency, unit price and unit distance loss rate of goods, as shown in Table 4. The unit distance cargo loss rate for each product is obtained by averaging the data over three random operating cycles.

Table 3
Basic parameters for warehouse operation

Parameters	Numeric value
M	5
B	15
L	15
l	1
h	1
w	1
v	1

Table 4
Cargo information

Cargo code	c_i	q_i	α_i	p_i
1	50	230	0.05	7
2	200	100	0.03	9
3	30	150	0.017	12
4	65	300	0.023	5
5	30	230	0.05	10
6	200	100	0.03	12
7	50	60	0.02	8
8	60	200	0.009	15
9	100	140	0.007	13
10	80	200	0.02	10

6.2 Feasibility Analysis

The solution obtained by using the solver CPLEX is an exact solution, while the solutions of heuristic algorithms are approximate. To compare the advantages and disadvantages of the solutions, the solver and the heuristic algorithms are used to solve the solution at the same scale (I=10) respectively. Table 5 shows the solution results of CPLEX 12.8.0, SPEA-II and NSGA-II algorithms. The Pareto frontiers obtained through the three methods are illustrated in Fig. 4.

Spread and hypervolume are commonly used multi-objective optimization evaluation metrics. The spacing method involves sorting the first objective function values of a set of solutions in ascending order and calculating the uniformity of the differences between adjacent sorted solutions. This metric reflects the uniformity of the distribution of solutions in the objective space. The specific calculation of this metric is shown in Equation (18), where N is the number of non-dominated solutions in the solution set, d_i is the Euclidean distance between two adjacent individuals in the non-dominated solution set, and d_f and d_l are the Euclidean distances between the extreme solutions and boundary solutions in the non-dominated solution set. A value of 0 for this metric indicates that all members of the Pareto optimal solutions are evenly distributed. The smaller the value, the better the distribution and diversity of the non-dominated solutions, and vice versa. The hypervolume method evaluates the quality of the solution set by calculating the volume of the objective space covered by the solution set. It measures the covered area in the objective space, with a larger hypervolume value indicating a greater coverage area and thus better quality of the solution set.

$$\Delta = \frac{d_f + d_l + \sum_{i=1}^{N-1} \left| d_i - \overline{d} \right|}{d_f + d_l + (N-1) \times \overline{d}} \tag{18}$$

Table 5
CPLEX and NSGA-II solution results

Methods	Optimal solutions	Solve time	Hypervolume	Spread
CPLEX	(571, 4.3) (582, 4.2) (588, 4.2) (594, 4.0)	11580	23.3	0.64
SPEA-II	(616, 4.6) (635, 4.5) (656, 4.4) (672, 4.3)	75	47.3	0.54
NSGA-II	(673, 4.9) (698, 4.8)	40	12.9	0.5

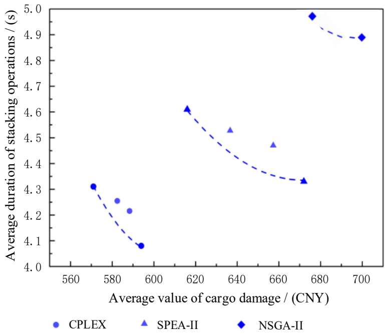

Fig. 4. The Pareto frontiers of CPLEX，SPEA-II and NSGA-II algorithms at the scale of I=10 (bidirectional motion mode)

The table results show minimal differences among the three solution methods for a limited scale of goods (I=10). However, CPLEX exhibits longer solving times compared to heuristic algorithms, NSGA-II and SPEA-II, which offer faster solutions despite being approximate. Among the three solutions, SPEA-II has the largest solution coverage, and its distribution is relatively uniform. Fig. 5(a), 5(b), and 5(c) depict commodity storage location distribution maps, randomly selected from solutions obtained by each algorithm. Due to the more types of goods, and each kind of goods only occupy a storage space, so this paper in the drawing of goods warehouse storage distribution map, each type of goods with and only with a color to indicate, but the same color may indicate different goods, so the storage distribution map only indicates the storage of goods but does not indicate the relationship between the types of goods.

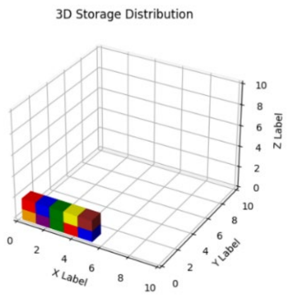

(a) result of CPLEX

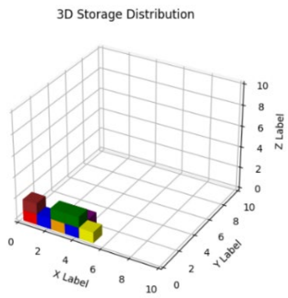

(b) result of SPEA-II

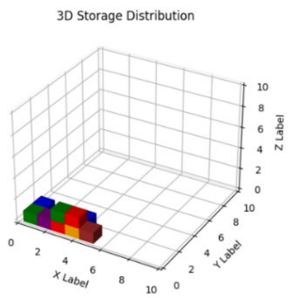

(c) result of NSGA-II

Fig. 5. The storage location distribution map at the scale of I=10

The storage distribution map offers valuable insights into the comparative results of CPLEX, SPEA-II, and NSGA-II. Obviously, there are notable differences in specific storage assignments for different commodities. These discrepancies contribute to variations in objective function values within the mathematical model.

5.3 Parameter Settings

For heuristic algorithms, performance is often sensitive to parameter settings, as different combinations directly affect both the efficiency and effectiveness of the algorithm's solution. To identify the most suitable parameter combinations for the current problem, this study employed orthogonal experimental design to systematically analyze the optimal values of key parameters in an improved genetic algorithm. This ensures that the algorithm can achieve optimal performance in practical applications. The performance of the genetic algorithm is mainly influenced by four parameters: population size, external archive size, crossover probability and mutation probability.

Therefore, 4 parameters and 4 levels are selected in this paper, so there are 16 groups of parameter combinations, as shown in Table 6 and 7.

Table 6
Parameter Levels

Parameters	Level 1	Level 2	Level 3	Level 4
	1	2	3	4
Population sizes	40	50	80	100
External archive sizes	10	20	30	40
Crossover probabilities	0.5	0.6	0.7	0.9
Genetic probabilities	0.05	0.1	0.2	0.3

Table 7
SPEA-II Algorithm Parameter Settings

Groups	Population sizes	External archive sizes	Crossover probabilities	Genetic probabilities
1	40	10	0.5	0.05
2	40	20	0.6	0.1
3	40	30	0.7	0.2
4	40	40	0.9	0.3
5	50	10	0.6	0.2
6	50	20	0.5	0.3
7	50	30	0.7	0.05
8	50	40	0.9	0.1
9	80	10	0.7	0.3
10	80	20	0.9	0.2
11	80	30	0.5	0.1
12	80	40	0.6	0.05
13	100	10	0.7	0.1
14	100	20	0.9	0.05
15	100	30	0.6	0.3
16	100	40	0.5	0.2

Run the code at each parameter level separately, and the solution results are shown in Table 8.

Table 8
Solution results for different groups of parameters

Groups	Solutions
1	(950,8.1)
2	(675,7.1),(680,6.2)
3	(720,6.3), (770,4.8)
4	(885,7.6), (1115,6.2), (1005,7.3), (1095,6.3)
5	(715,6.9), (780,6.6)
6	(800,6.3)
7	(775,5.2), (680,5.4)
8	(616,4.6), (635,4.6), (656,4.4), (672,4.3)
9	(760,6.3), (700,6.5)
10	(710,5.4)
11	(900,6.6), (825,6.8)
12	(755,5.9), (760,5.8), (805,5.6)
13	(735, 6.4)
14	(1180, 6.5), (825,10.4), (820,11.1)
15	(1085,6.0), (890, 6.5), (1060, 6.1)
16	(645, 5.1) (615, 5.6)

The set coverage method is a metric used to evaluate the performance of multi-objective optimization algorithms by measuring the extent to which one solution set covers another. The formula for its calculation is:

$$C(A,B)=\frac{\left|\{b\in B\mid \exists a\in A, a\succ b\}\right|}{|B|} \tag{19}$$

This formula represents the coverage ratio of set A over set B, which is the number of solutions in set B that are dominated by at least one solution in set A, divided by the total number of solutions in set B. By calculating the proportion of solutions in set B that are covered by in set A, the set coverage method provides an intuitive and easy-to-calculate way to compare the effectiveness of different algorithms in solving multi-objective optimization problems. Table 9 shows the set coverage values obtained by comparing the two sets of data, the larger the total set coverage value corresponding to the solution result of each set of parameters, the fewer solutions that govern the set of solutions, and the better the set of solutions.

Table 9
Set coverage matrix of different parameter groups

Groups	1	2	3	4	5	6	7	8	9	10	11	12	13	14	15	16	Total
1	—	0	0	0	0	0	0	0	0	0	0	0	0	0	0	0	0
2	1	—	0.5	1	1	1	0	0	1	0	1	0	1	1	0.3	0	8.8
3	1	0	—	0	0	0	0	0	0	0	0	0	0	0.3	0	0	1.3
4	1	0	0	—	0	0	0	0	0	0	0	0	0	0.3	0	0	1.3
5	1	0	0	0.5	—	0	0	0	0	0	0	0	0	0.7	0	0	2.2
6	1	0	0	0.8	0	—	0	0	0	0	1	0	0	1	0.3	0	4.1
7	1	0.5	0.5	1	1	1	—	0	1	1	1	1	1	1	1	0	12
8	1	1	1	1	1	1	1	—	1	1	1	1	1	1	1	0.5	14.5
9	1	0	0	0.8	1	1	0	0	—	0	1	0	0	1	0.3	0	6.1
10	1	0	0.5	1	1	1	0	0	0.5	—	1	1	1	1	1	0	10
11	1	0	0	0.5	0	0	0	0	0	0	—	0	0	0.3	0	0	1.8
12	1	0	0	1	0.5	1	0	0	0.5	0	1	—	0	1	1	0	7
13	1	0	0	0.5	0.5	0	0	0	0	0	1	0	—	1	0.3	0	4.3
14	0	0	0	0	0	0	0	0	0	0	0	0	0	—	0	0	0
15	1	0	0	0.8	0	0	0	0	0	0	0.5	0	0	0.3	—	0	2.6
16	1	1	0.5	1	1	1	1	0	1	1	1	1	1	1	0	—	12.5

As can be seen from Fig. 6, group 8 corresponds to the largest value, so the final parameter selection of the SPEA-II algorithm is shown in Table 10.

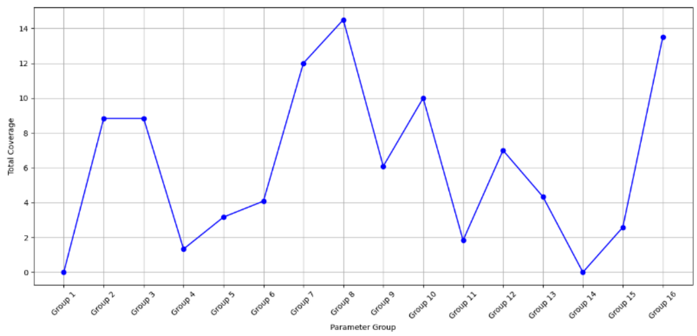

Fig. 6. The total coverage value of different parameter groups

Table 10
Algorithm optimal parameter settings

Parameters	Numeric value
Number of iterations	400
Population size	50
External archive size	40
Crossover probability	0.9
Genetic probability	0.1

6.4 Sensitivity analysis

6.4.1 Comparison of solution results at different scales

To assess the performance of the SPEA-II algorithm, a range of studies were randomly generated. Given the CPLEX solver's limitations for scales beyond 10, SPEA-II's results were benchmarked against random solutions and the NSGA-II algorithm. Information on goods of small, medium and large sizes is shown in the first 20, 50 and 100 rows of Table 11, respectively. The results of the solution are recorded in Table 12 and 13. Fig. 7, 8, 9 and 10 visually analyze the Pareto frontiers across scales, providing a comprehensive overview. Representative solutions from both algorithms' Pareto sets are selected, with cargo layout diagrams depicted in Fig. 8, 9, and 10 (subfigures (a) and (b)), facilitating the evaluation of algorithm effectiveness across different cargo scales.

Table 11
Cargo information

Cargo code	c_i	q_i	α_i	p_i
1	50	230	0.05	7
2	200	100	0.03	9
3	30	150	0.017	12
4	65	300	0.023	5
5	30	230	0.05	10
6	200	100	0.03	12
7	50	60	0.02	8
8	60	200	0.009	15
9	100	140	0.007	13
10	80	200	0.02	10
11	65	100	0.04	12
12	70	120	0.01	5
13	30	40	0.02	7
14	50	70	0.01	4
15	25	150	0.03	5
16	80	55	0.027	8
17	180	60	0.023	10
18	200	85	0.005	6
19	140	40	0.06	6
20	50	200	0.04	3
21	119	370	0.004	2
22	246	372	0.04	23
23	78	228	0.003	22
24	94	69	0.009	13
25	245	374	0.003	10
26	171	236	0.001	7
27	129	213	0.008	23
28	200	78	0.005	12
29	287	357	0.007	11
30	281	384	0.001	7
31	163	235	0.002	2
32	110	347	0.006	11
33	94	314	0.003	6
34	298	127	0.007	10
35	235	201	0.007	25
36	132	121	0.007	6
37	230	259	0.009	18
38	142	293	0.009	7
39	261	289	0.005	12
40	73	296	0.003	21
41	104	389	0.01	15
42	90	377	0.003	23
43	238	192	0.002	12
44	163	233	0.004	24
45	178	94	0.006	24
46	48	253	0.006	14
47	35	59	0.001	5
48	250	99	0.005	18
49	146	156	0.03	4
50	171	391	0.009	6
51	119	339	0.005	6
52	49	117	0.004	11
53	247	60	0.009	21
54	169	131	0.007	9
55	243	60	0.008	11
56	61	372	0.008	15
57	116	194	0.008	11
58	191	181	0.01	8
59	114	126	0.006	16
60	274	60	0.002	9
61	71	347	0.005	8
62	45	287	0.005	11
63	186	375	0.010	7
64	291	309	0.004	15
65	222	395	0.004	18
66	114	162	0.005	16
67	223	340	0.01	15
68	240	129	0.006	8
69	294	273	0.003	23
70	214	361	0.03	25
71	207	343	0.007	11
72	210	208	0.009	16

Table 11
Cargo information (Continued)

Cargo code	c_i	q_i	α_i	p_i
73	211	144	0.006	16
74	220	206	0.004	12
75	269	301	0.005	3
76	22	195	0.004	14
77	43	264	0.007	8
78	198	261	0.006	6
79	30	146	0.009	21
80	198	134	0.002	22
81	262	391	0.002	22
82	268	359	0.009	24
83	195	323	0.005	16
84	43	111	0.002	4
85	70	313	0.005	19
86	50	233	0.008	15
87	278	272	0.05	5
88	167	131	0.002	4
89	234	245	0.004	21
90	60	86	0.002	5
91	103	258	0.002	15
92	26	334	0.005	20
93	150	75	0.002	16
94	174	150	0.005	16
95	241	80	0.004	17
96	113	206	0.02	21
97	191	104	0.004	13
98	285	350	0.008	9
99	69	143	0.006	20
100	268	176	0.006	8

Table 12
Results of solutions at different scales

Scales	Solution results	Optimal solutions	Solve time	Hypervolume	Spread
small-scale (I=20)	Random	（4933, 32.7）	77	19.4	1
	SPEA-II	（944, 8.1） （985, 7.9） （1006, 7.9）	35	214.3	0.66
	NSGA -II	（1062, 9.4） （1157, 9.2） （1172, 8.1）	130	122.2	0.86
medium-scale (I=50)	Random	（6796, 45.1）	120	3.28	1
	SPEA-II	（1053, 8.2） （1118, 8.2）	340	264	0.5
	NSGA-II	（2430, 15.9） （2752, 15.8）	270	41.8	0.5
large-scale (I=100)	Random	（10032, 84.0）	225	65.96	1
	SPEA-II	（2119, 15.3） （2255, 15.1） （3125, 14.9）	1370	905.7	0.86
	NSGA-II	（3195, 22.0） （3175, 20.7） （3328, 20.5）	450	243	0.88

Table 13
Domination relationship between solution sets from different algorithms

Scales	Methods	Random	SPEA-II	NSGA-II
small-scale (I=20)	Random	——	0.00	0.00
	SPEA-II	1.00	——	1.00
	NSGA-II	1.00	0.00	——
medium-scale (I=50)	Random	——	0.00	0.00
	SPEA-II	1.00	——	1.00
	NSGA-II	1.00	0.00	——
large-scale (I=100)	Random	——	0.00	0.00
	SPEA-II	1.00	——	1.00
	NSGA-II	1.00	0.00	——

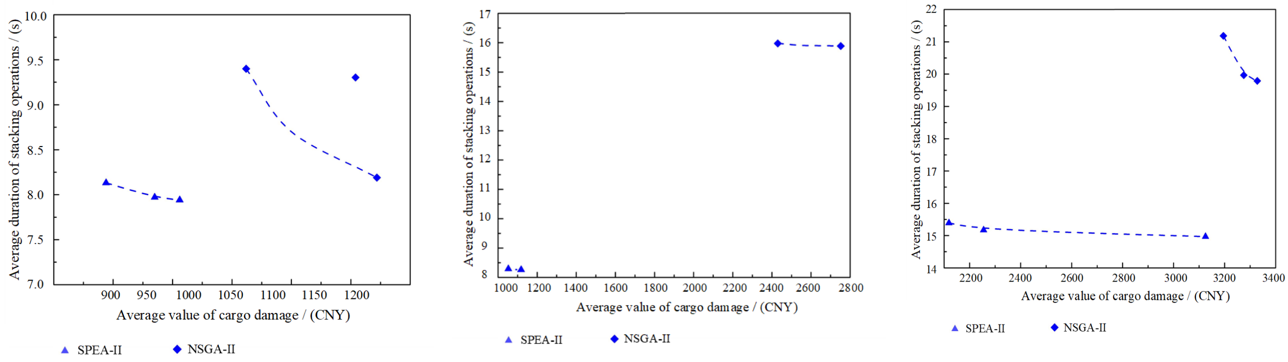

(a) I=20 (b) I=50 (c) I=100

Fig. 7. The Pareto frontiers of the SPEA-II and NSGA-II algorithms under different cargo scales

It can be seen that SPEA-II has always positioned its leading edge below NSGA-II, and its solution has better distribution uniformity while covering a larger space range, which highlights the superior performance of this algorithm in different problem scales. However, this increase in performance is accompanied by longer computation times, raising questions about algorithm efficiency and computational resource optimization at different scales.

(a) result of SPEA-II (b) result of NSGA-II

Fig. 8. The storage location distribution map at the scale of I=20

(a) result of SPEA-II (b) result of NSGA-II

Fig. 9. The storage location distribution map at the scale of I=50

(a) result of SPEA-II (b) result of NSGA-II

Fig. 10. The storage location distribution map at the scale of I=100

The SPEA-II algorithm corresponds to a storage location distribution map in which the goods are stored more centrally and closer to the starting point of the stacker. Table 12 and 13 further illustrates significant differences in objective function values between the two algorithms.

6.4.2 Comparison of solution results at different shelf rows scales

To assess the effect of shelf size on stacker operation time and damage cost, storage allocation is conducted with 5 and 10 shelves. At M=10, CPLEX, SPEA-II, and NSGA-II yield the optimal solution (523, 3.5). Further comparison is made for I=20. Table 14 and 15 summarizes the results, and Fig. 11 depicts Pareto frontiers and storage layouts. Fig. 12 shows storage layouts obtained by all methods. Fig. 13(a) and 13(b) display storage allocation maps for SPEA-II and NSGA-II solutions with 20 cargo types and 10 shelves.

Table 14
Results of solutions under different shelf scales

Scales	Methods	Optimal solutions (M=5)	Optimal solutions (M=10)	Hypervolume (M=5/ M=10)	Spread (M=5/ M=10)
super small-scale (I=10)	Random	（3240, 25.0）	（2422, 19.8）	58.8/13.3	1/1
	CPLEX	(571, 4.3) (582, 4.2) (588, 4.2) (594, 4.0)	(523, 3.5)	43.3/35	0.64/1
	SPEA-II	(616, 4.6) (635, 4.5) (656, 4.4) (672, 4.3)	(523, 3.5)	33.3/35	0.54/1
	NSGA-II	(673, 4.9) (698, 4.8)	(523, 3.5)	2.9/35	0.50/1
small-scale (I=20)	Random	（4933, 32.7）	（3422, 28.9）	19.43/80.34	1/1
	CPLEX	——	——	——	——
	SPEA-II	（944, 8.1） （985, 7.9） （1006, 7.9）	（638, 5.8） （663, 5.7） （676, 5.7） （685, 5.5） （725, 5.5）	37.4/44.1	0.66/0.75
	NSGA-II	（1062, 9.4） （1157, 9.2） （1172, 8.1）	（976, 8.3） （1047, 7.8） （1086, 7.7）	122.2/468.7	0.86/0.64

Table 15
Set coverage of different algorithms under different scales

		M=5				M=10			
Scales	Methods	Random	CPLEX	SPEA-II	NSGA-II	Random	CPLEX	SPEA-II	NSGA-II
super small-scale (I=10)	Random	——	0.00	0.00	0.00	——	0.00	0.00	0.00
	CPLEX	1.00	——	1.00	1.00	1.00	——	1.00	1.00
	SPEA-II	1.00	0.00	——	1.00	1.00	0.00	——	1.00
	NSGA-II	1.00	0.00	0.00	——	1.00	0.00	0.00	——
small-scale (I=20)	Random	——	——	0.00	0.00	——	——	0.00	0.00
	CPLEX	——	——	——	——	——	——	——	——
	SPEA-II	1.00	——	——	1.00	1.00	——	——	1.00
	NSGA-II	1.00	——	0.00	——	1.00	——	0.00	——

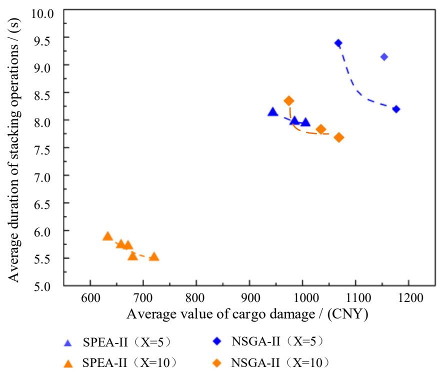

Fig. 11. The Pareto frontiers of the SPEA-II and NSGA-II algorithms under different shelf row scales

As the number of shelves increases at the same cargo size, the objective function value decreases. Moreover, with 10 shelves, solutions from the SPEA-II algorithm significantly improve compared to the case with 5 shelves. Thus, constructing an appropriate number of shelves according to incoming goods scale can enhance warehouse operation efficiency.

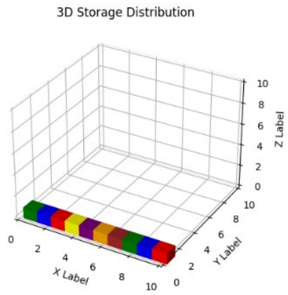

Fig. 12. The storage location distribution map at the scale of I=10 and M=10

(a) result of SPEA-II

(b) result of NSGA-II

Fig. 13. The storage location distribution map at the scale of I=20 and M=10

Fig. 13(a) shows a more concentrated distribution of cargo storage locations, strategically positioned closer to the stacker entrance and exit. This concentration indicates a potentially more efficient storage arrangement, crucial for warehouse logistics.

6.4.3 Comparison of solution results in different stacker crane operating modes

This paper examines the impact of unidirectional and bidirectional concurrent motion modes on stacker crane operation and warehouse efficiency using CPLEX in a super small-scale optimization (I=10). Table 16, 17 and Fig. 14 present the results. Fig. 15(a) and 15(b) depict storage location distribution maps for unidirectional motion mode using SPEA-II and NSGA-II algorithms at I=10 and M=5, respectively. Traversal time in stacker crane operation, disregarding acceleration and deceleration time, is the sum of horizontal and vertical temporal expenditures. Effective displacement is the combination of distances along both axes. Eq. (3) in Section 3 is revised to Eq. (20) under unchanged formulas and constraints.

$$d_{oi} = y_i \times l + (z_i - 1) \times h \tag{20}$$

Table 16
Results of solutions under different stacker crane operation modes

Methods	Optimal solutions (Bidirectional motion mode)	Optimal solutions (Unidirectional motion mode)	Hypervolume (Bidirectional/ Unidirectional)	Spread (Bidirectional/ Unidirectional)
CPLEX	(571, 4.3) (582, 4.2) (588, 4.2) (594, 4.0)	(665, 5.2) (686, 5.1) (710, 5.1) (714, 5.0) (752, 4.9) (758, 4.9) (792, 4.9)	23.3/65.3	0.65/0.76
SPEA-II	(616, 4.6) (635, 4.5) (656, 4.4) (672, 4.3)	(935, 7.6) (1075, 6.8) (1188, 6.7) (1271, 6.4)	47.3/345.9	0.55/0.59
NSGA-II	(673, 4.9) (698, 4.8)	(995,7.4) (1104,7,3) (1143,7.0)	2.9/119.7	0.50/0.74

Table 17
Set coverage of different algorithms under from different motion mode

	Bidirectional motion mode			Unidirectional motion mode		
	CPLEX	SPEA-II	NSGA-II	CPLEX	SPEA-II	NSGA-II
CPLEX	——	1.00	1.00	——	1.00	1.00
SPEA-II	0.00	——	1.00	0.00	——	1.00
NSGA-II	0.00	0.00	——	0.00	0.00	——

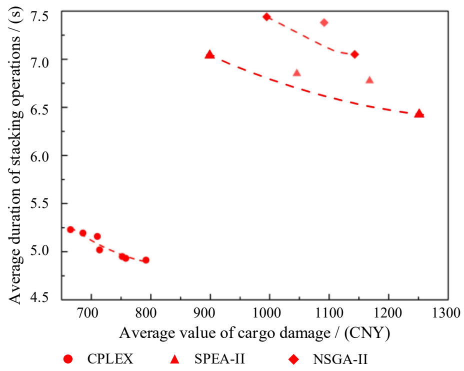

Fig. 14. The Pareto frontiers of the SPEA-II and NSGA-II algorithms at the scale of I=10 (unidirectional motion mode)

The comparison between unidirectional (Fig. 4) and bidirectional (Fig. 14) movement patterns and the two tables above reveal a substantial difference in objective function values. Unidirectional motion enhances load stability. Conversely, bidirectional concurrent motion notably improves operational efficiency and reduces per-unit cargo damage costs. This underscores the intricate balance between load stability, operational efficiency, and cargo damage costs.

(a) result of SPEA-II (b) result of NSGA-II

Fig. 15. The storage location distribution map at the scale of I=20 and M=10 (unidirectional motion mode)

The findings from Fig. 15 and Table 16 and 17 confirm the superior solving efficacy of SPEA-II over NSGA-II. SPEA-II's impact extends beyond Pareto frontier positioning to measurable performance metrics, consistently delivering higher solution quality and optimal cargo storage configuration.

7. Conclusions and future works

This study employs a novel approach, focusing on warehouse operations from the perspective of warehouse managers by analyzing key factors affecting efficiency: operational efficiency and cargo loss. The warehouse allocation model analyzes these two key indicators simultaneously to improve the overall performance of the warehouse. Additionally, it selectively extracts a subset from the Pareto solution set to generate a distribution layout diagram of storage locations. The study constructs Pareto frontiers to visually delineate the trade-offs between operational efficiency and goods loss. The research results of this paper show that whether the distribution of storage space in the warehouse is reasonable or not will have a significant impact on the operation efficiency of the warehouse and the loss caused by the movement of goods. Unreasonable storage space layout will make the enterprise respond to customer demand for a longer time, and at the same time, the warehouse operation cost will also increase. Therefore, enterprises should start from the overall perspective. Not only should we focus on operational efficiency, we should also consider the cost, so as to obtain more benefits and improve the overall competitiveness of the warehouse. In addition, through the comparison of different shelf size, stacker operation mode and cargo size, it is found that although the single direction of operation is more stable, the operation mode of two directions at the same time can effectively improve the operation efficiency and reduce cargo damage. And with the increase in the size of the goods, the appropriate expansion of the size of the shelf can make the storage allocation significantly optimized, but the inconsistency between the size of the warehouse and the size of the goods may also lead to the waste of storage space. The results of this paper also verify the effectiveness of SPEA-II algorithm in solving storage allocation problems from the aspects of objective function value, solution coverage size and distribution uniformity.

Future research could delve deeper into integrating a comprehensive framework that accounts for the intricate interplay between goods during both inbound and outbound processes. Additionally, exploring the dynamic nature of the storage lifecycle, with an emphasis on developing adaptive algorithms capable of accommodating evolving demands and optimizing warehouse performance, holds significant promise. Addressing these nuances will contribute to a more nuanced and holistic understanding of warehouse management systems, thereby facilitating enhanced operational efficiency and strategic decision-making within the logistics domain.

Acknowledgements

The authors would like to express their gratitude for the financial support provided by the National Natural Science Foundation of China (Project No. 72204034; Project No. 72174035), the China Postdoctoral Science Foundation (Project No. 2024T170083), the General Project of the China Postdoctoral Science Foundation (Project No. 2023M730457), the Fundamental Research Funds for the Central Universities (Project No. 3132024293; Project No. 3132023526), and the Liaoning Provincial Social Science Planning Fund Project (Project No. L21CGL006).

Disclosure Statement

The authors declare that we do not have any commercial or associative interest that represents a conflict of interest in connection with the work submitted.

References

Abdirad, M., & Krishnan, K. (2021). Industry 4.0 in logistics and supply chain management: a systematic literature review. *Engineering Management Journal*, *33*(3), 187-201.

Accorsi, R., Manzini, R. & Maranesi, F. (2014). A decision-support system for the design and management of warehousing systems. *Computers in Industry*, *65*(1), 175–186.

Accorsi, R., Manzini, R., & Bortolini, M. (2012). A hierarchical procedure for storage allocation and assignment within an order-picking system. A case study. *International Journal of Logistics Research and Applications*, *15*(6), 351-364.

Bartholdi, J. J., & Hackman, S. T. (2008). *Warehouse & Distribution Science: Release 0.89* (p. 13). Atlanta: Supply Chain and Logistics Institute.

Bozer, Y. A., & Aldarondo, F. J. (2018). A simulation-based comparison of two goods-to-person order picking systems in an online retail setting. *International Journal of Production Research*, *56*(11), 3838-3858.

Chiu, S., Huang, Y., Chiu, Y & Chiu, T. (2019). Satisfying multiproduct demand with a FPR-based inventory system featuring expedited rate and scraps. *International Journal of Industrial Engineering Computations, 10*(3), 443-452.

Esmer, S., Yildiz, G., & Tuna, O. (2013). A new simulation modelling approach to continuous berth allocation. *International Journal of Logistics Research and Applications*, *16*(5), 398-409.

Francis, R.L., McGinnis, L.F. & White, J.A. (1992). *Facility layout and location: an analytical approach.* 2nd ed., Englewood Cliffs, N. J.

Franzke, T., Grosse, E. H., Glock, C. H., & Elbert, R. (2017). An investigation of the effects of storage assignment and picker routing on the occurrence of picker blocking in manual picker-to-parts warehouses. *The International Journal of Logistics Management*, *28*(3), 841-863.

Frazelle, E. (2002). *World-class warehousing and material handling*. Boston, MA.

Frazelle, E.H. (2000). *Trends in transportation, Logistics Management Series.* Atlanta, GA.

Grosse, E. H., Glock, C. H., Jaber, M. Y., & Neumann, W. P. (2015). Incorporating human factors in order picking planning models: framework and research opportunities. *International Journal of Production Research*, *53*(3), 695-717.

Guan, M., & Li, Z. (2018). Genetic Algorithm for scattered storage assignment in Kiva mobile fulfillment system. *American Journal of Operations Research*, *8*(6), 474-485.

Guerriero, F., Pisacane, O. & Rende, F. (2015). Comparing heuristics for the product allocation problem in multi-level warehouses under compatibility constraints. *Applied Mathematical Modelling*, 39(23-24). 7375-7389.

Hohmann, N., Bujny, M., Adamy, J., & Olhofer, M. (2022, July). Multi-objective 3D path planning for UAVS in large-scale urban scenarios. In *2022 IEEE Congress on Evolutionary Computation (CEC)* (pp. 1-8). IEEE.

Hoshimov, A., Cagliano, A. C., Mangano, G., Schenone, M., & Grimaldi, S. (2024). AS/R system travel time in class-based storage with different input-output point levels: a proposed formula. *Journal of Facilities Management*, *22*(1), 108-123.

Jiao, S., Wang, X., Ma, C., & Deng, Y. (2024). How does sports e-commerce influence consumer behavior through short video live broadcast platforms? Attachment theory perspective. *Asia Pacific Journal of Marketing and Logistics*.

Lagorio, A., Di Pasquale, V., Cimini, C., Miranda, S., & Pinto, R. (2022). Augmented Reality in Logistics 4.0: implications for the human work. *IFAC-PapersOnLine*, *55*(10), 329-334.

Lam, C.H.Y., Choy, K.L. & Chung, S.H. (2010). Framework to measure the performance of warehouse operations efficiency. *2010 8th IEEE International Conference on Industrial Informatics*, 634-639.

Lee, I. G., Chung, S. H., & Yoon, S. W. (2020). Two-stage storage assignment to minimize travel time and congestion for warehouse order picking operations. *Computers & industrial engineering*, *139*, 106129.

Li, J., Huang, R., & Dai, J. B. (2017a). Joint optimisation of order batching and picker routing in the online retailer's warehouse in China. *International Journal of Production Research*, *55*(2), 447-461.

Li, Z.P., Zhang, J.L., Zhang, H.J. & Hua, G.W. (2017b). Optimal selection of movable shelves under cargo-to-person picking mode. *International Journal of Simulation Modelling*, *16*(1), 145-156.

Liu, C., Gong, Z., Teo, K. L., & Feng, E. (2016). Multi-objective optimization of nonlinear switched time-delay systems in fed-batch process. *Applied Mathematical Modelling*, *40*(23-24), 10533-10548.

Liu, J., Liao, H., & White Jr, J. A. (2021). Stochastic analysis of an automated storage and retrieval system with multiple in-the-aisle pick positions. *Naval Research Logistics (NRL)*, *68*(4), 454-470.

Liu, M., & Poh, K. L. (2023). E-commerce warehousing: An efficient scattered storage assignment algorithm with bulky locations. *Computers & Industrial Engineering*, *181*, 109236.

Liu, T., Gong, Y. & De Koster, R.B.M. (2018). Travel time models for split-platform automated storage and retrieval systems. *International Journal of Production Economics*, *197*, 197-214.

Lütke Entrup, M., Günther, H. O., Van Beek, P., Grunow, M., & Seiler, T. (2005). Mixed-Integer Linear Programming approaches to shelf-life-integrated planning and scheduling in yoghurt production. *International journal of production research*, *43*(23), 5071-5100.

Manzini, R. (2012). *Warehousing in the global supply chain: advanced models, tools and applications for Storage Systems*. Springer, London.

Maxim, A.D., Eren, E.O., Ren, M. & Mehmer, B.U. (2016). Intermodal freight network design for transport of perishable products. *Open Journal of Optimization*, *5*(4), 120-139.

Mirzaei, M., Zaerpour, N., & De Koster, R. (2021). The impact of integrated cluster-based storage allocation on parts-to-picker warehouse performance. *Transportation Research Part E: Logistics and Transportation Review*, *146*, 102207.

Moon, G. & Kim, G.P. (2001). Effects of relocation to AS/RS storage location policy with production quantity variation. *Computers & Industrial Engineering*, *40*(1), 1-13.

Myers, D.C. (1997). Meeting seasonal demand for products with limited shelf lives. *Naval Research Logistics*, *44*, 473-483.

Ozden, S.G., Smith, A.E., & Gue, K.R. (2020). A novel approach for modeling order picking paths. *Naval Research Logistics, 68*, 471- 484.

Pawar, N.S., Rao, S.S. & Adil, G.K. (2022). A new measure for scattering of stocks in e-commerce warehouses", *IFAC PapersOnLine*, *55*(10), 1357-1362.

Rong, A.Y., Renzo, A. & Martin, G. (2011). An optimization approach for managing fresh food quality throughout the supply chain. *Production Economics*, *131*(1), 421-429.

Rose, S., Gopal, P.R.C. & Arputham, R.M. (2021). Operational efficiency of tow trucks: a case based evidence from an Indian automobile manufacturer. *Journal of Facilities Management*, *19*(3), 304-326.

Samira, K. (2022). Sustainability balanced scorecard approach to internet of things enabled logistics systems", *Engineering Management Journal*, *34*(3), 450-474.

Sari, Z., Grasman, S.E. & Ghouali, N. (2007). Impact of pickup/delivery stations and restoring conveyor locations on retrieval time models of flow-rack automated storage and retrieval systems. *Production Planning and Control*, *18*(2), 105-116.

Silva, A., Coelho, L. C., Darvish, M., & Renaud, J. (2020). Integrating storage location and order picking problems in warehouse planning. *Transportation Research Part E: Logistics and Transportation Review*, *140*, 102003.

Tokat, S., Karagul, K., Sahin, Y., & Aydemir, E. (2022). Fuzzy c-means clustering-based key performance indicator design for warehouse loading operations. *Journal of King Saud University Computer and Information Sciences*, *34*(8), 6377-6384.

Tompkins, J.A., White, J.A., Bozer, Y.A. & Tanchoco, J.A. (2010). *Facilities Planning*. Wiley, New York, NY.

Van Gils, T., Caris, A., Ramaekers, K., & Braekers, K. (2019). Formulating and solving the integrated batching, routing, and picker scheduling problem in a real-life spare parts warehouse. *European Journal of Operational Research*, *277*(3), 814-830.

Womack, J. P., Jones, D. T., & Roos, D. (2007). *The machine that changed the world: The story of lean production--Toyota's secret weapon in the global car wars that is now revolutionizing world industry*. Simon and Schuster.

Xiang, X., Liu, C., & Miao, L. (2018). Storage assignment and order batching problem in Kiva mobile fulfilment system. *Engineering Optimization*, *50*(11), 1941-1962.

Xiao, J., & Zheng, L. (2012). Correlated storage assignment to minimize zone visits for BOM picking. *The International Journal of Advanced Manufacturing Technology*, *61*(5), 797-807.

Yang, C. L., & Nguyen, T. P. Q. (2016). Constrained clustering method for class-based storage location assignment in warehouse. *Industrial Management & Data Systems*, *116*(4), 667-689.

Yang, P., Zhao, Z., & Guo, H. (2020). Order batch picking optimization under different storage scenarios for e-commerce warehouses. *Transportation Research Part E: Logistics and Transportation Review*, *136*, 101897.

Zhang, H & Shi, F. (2024). A multi-objective site selection of electric vehicle charging station based on NSGA-II. *International Journal of Industrial Engineering Computations, 15*(1), 293-306.

Zhang, J., Liu, F., Tang, J. & Li, Y.H. (2019). The online integrated order picking and delivery considering picker's learning efforts for an O2O community supermarket. *Transportation Research Part E-Logistics and Transportation Review*, *123*(11), 180-199.

Zhang, J.R., Sevilay, O. & Sanchoy, D. (2020). The dynamic stocking location problem – Dispersing inventory in fulfillment warehouses with explosive storage. *International Journal of Production Economics*, 224, 107550-107550.

Zhong, S.Z., Vaggelis, G., Jorge, M., Duncan, M., Cheng, J. & Shao, W. (2022). Evaluating the benefits of picking and packing planning integration in e-commerce warehouses. *European Journal of Operational Research*, *301*(1), 67-81.